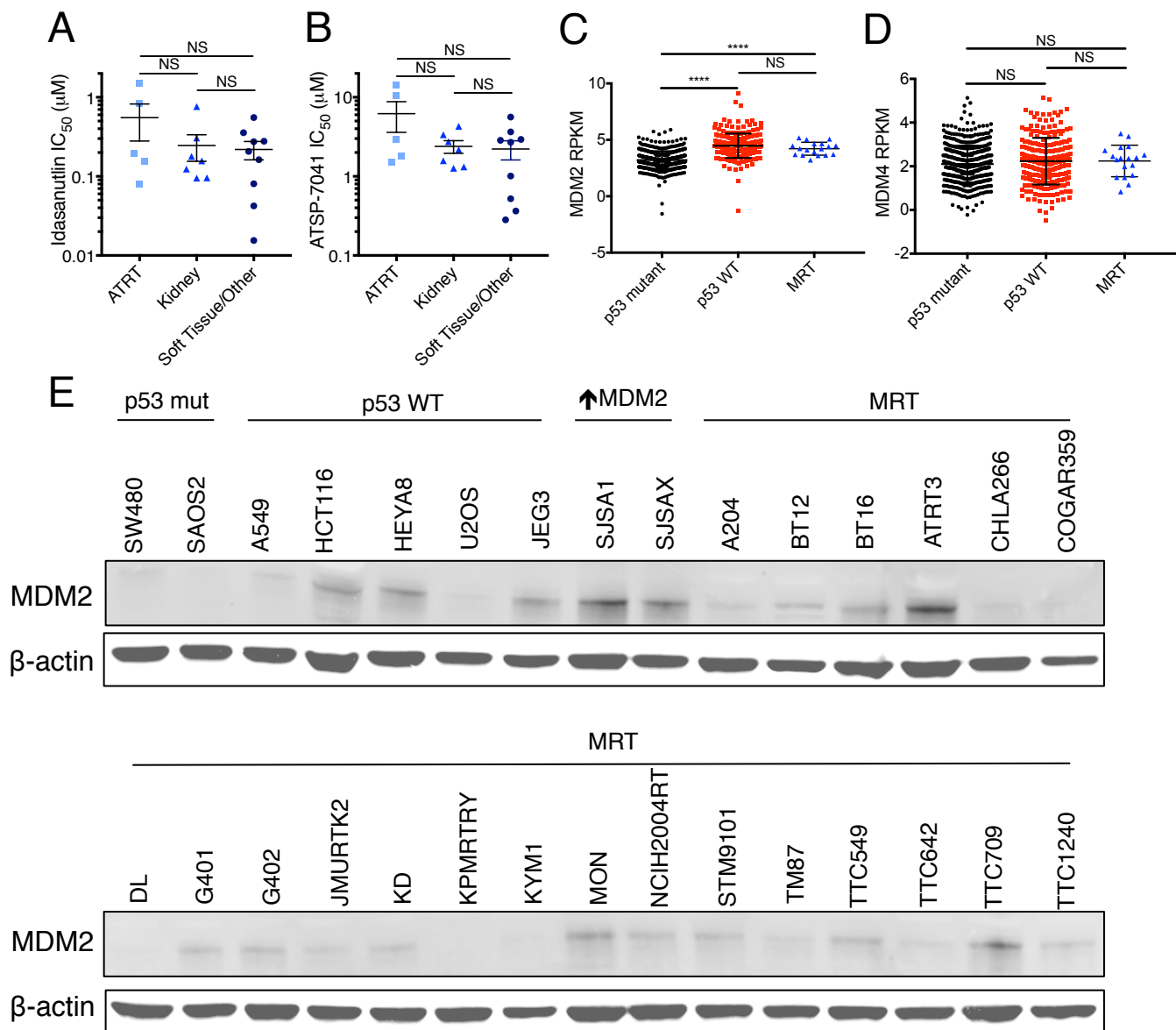
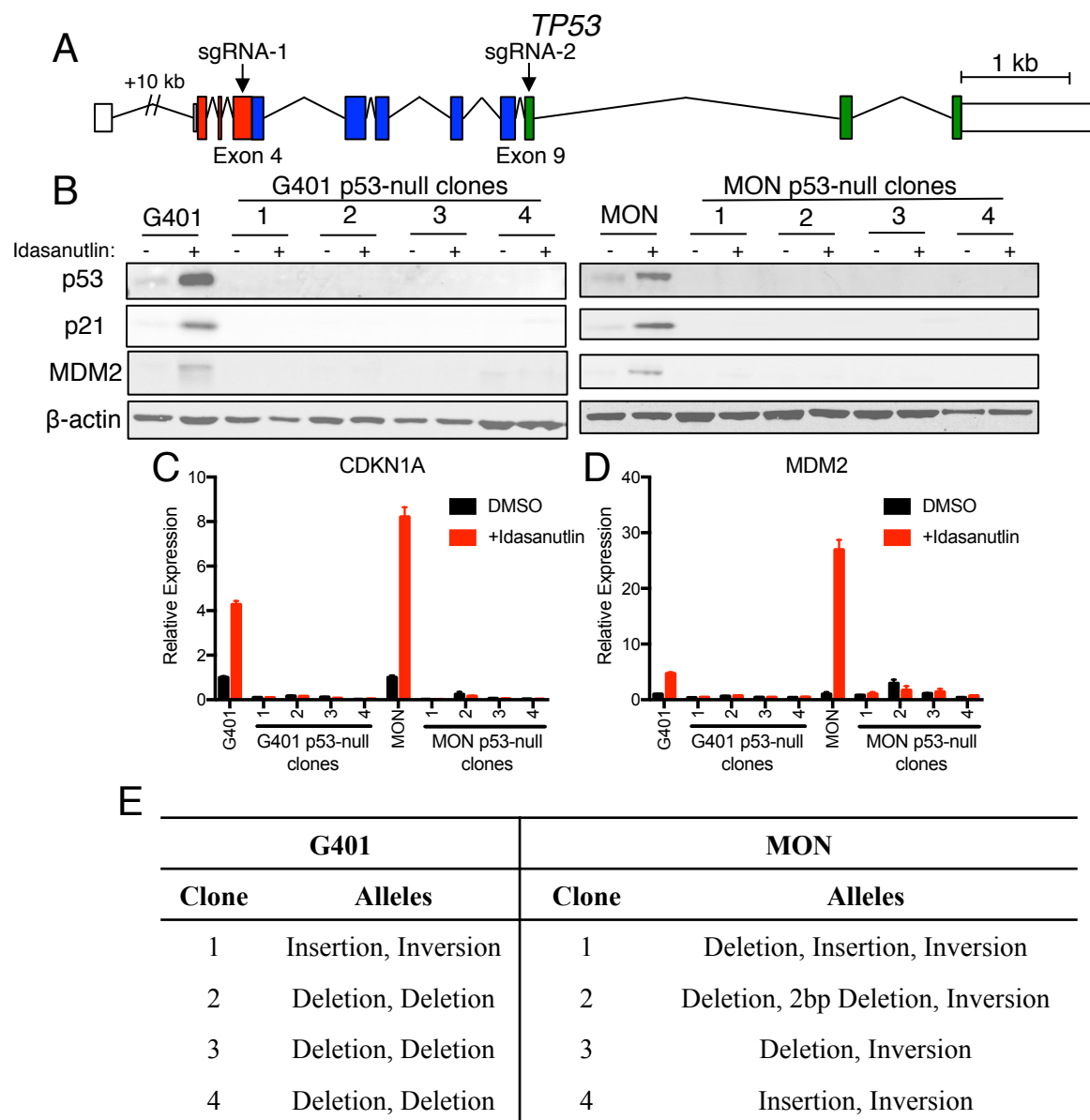


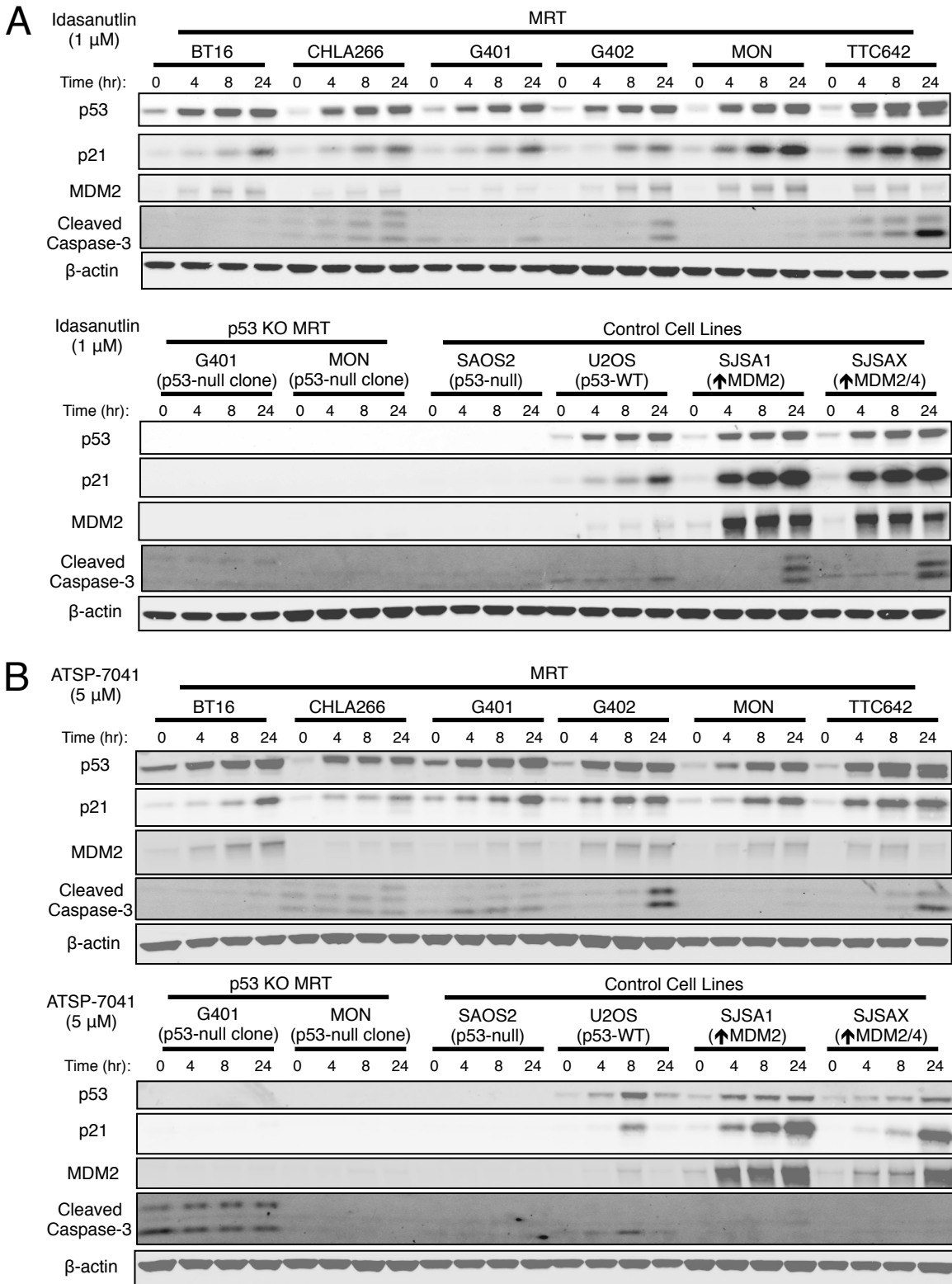
Supplementary Figure 1. MRT cell lines are more sensitive to genetic perturbations of the p53 pathway than other p53 WT cell lines. (A) Genome-scale RNAi screens of 10 MRT cell lines and 491 other cancer cell lines, as plotted in Figure 1A. (B-F) Distribution of CRISPR-Cas9 screen dependency scores for *MDM2* (B), *MDM4* (C), *TP53* (D), *PPM1D* (E), and *USP7* (F). Each point represents one cell line and data show mean \pm SD. Negative dependency scores indicate that the particular cell line was more vulnerable to sgRNAs targeting the indicated gene while positive dependency scores suggest that the sgRNAs increased cell number. p53 statuses were determined using mutational calls and gene expression signatures (Methods, Supplementary Table S2). Significance calculated by one-way ANOVA with Holm-Sidak's multiple comparisons correction. * - $P < 0.05$; ** - $P < 0.01$; *** - $P < 0.001$; **** - $P < 0.0001$.



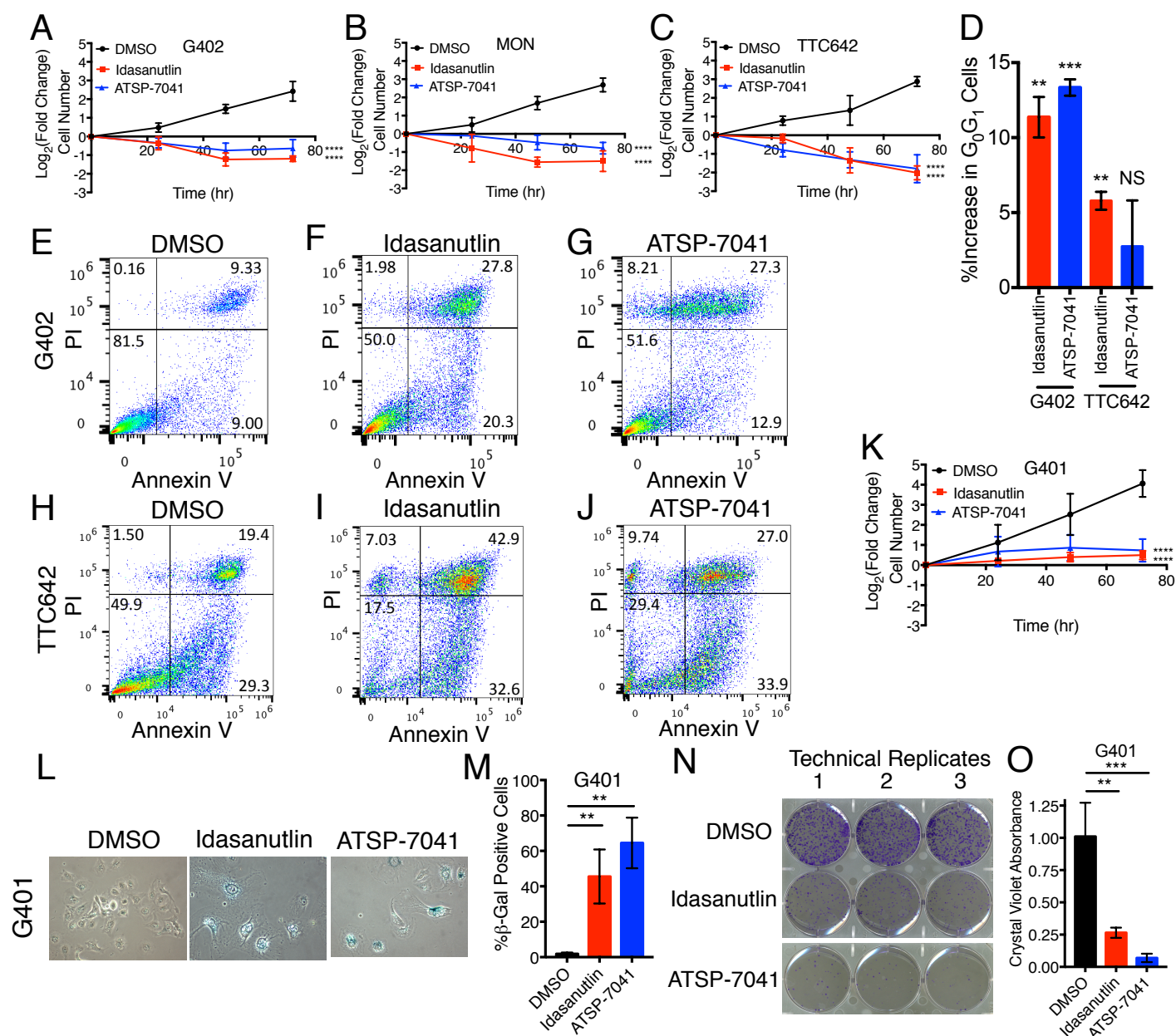
Supplementary Figure 2. MRT location and MDM2/4 expression does not explain differential sensitivity to MDM2 and MDM2/4 inhibition. (A-B) IC_{50} for idasanutlin (A) and ATSP-7041 (B) in each cell line as indicated in Figure 2A,C with MRT lines segregated by the anatomical location of the tumors from which the cell lines were derived. Data show mean \pm SEM. Significance calculated by one-way ANOVA with Holm-Sidak's multiple comparisons correction. (C-D) RNA-seq expression values in Reads per Kilobase Million (RPKM) for MDM2 (C) and MDM4 (D) of various cell lines in the Cancer Cell Line Encyclopedia. Each point represents one cell line. Error bars show mean \pm SD. Significance calculated by one-way ANOVA with Holm-Sidak's multiple comparisons correction. (E) Immunoblot for baseline MDM2 expression in all cell lines used in Figure 2.



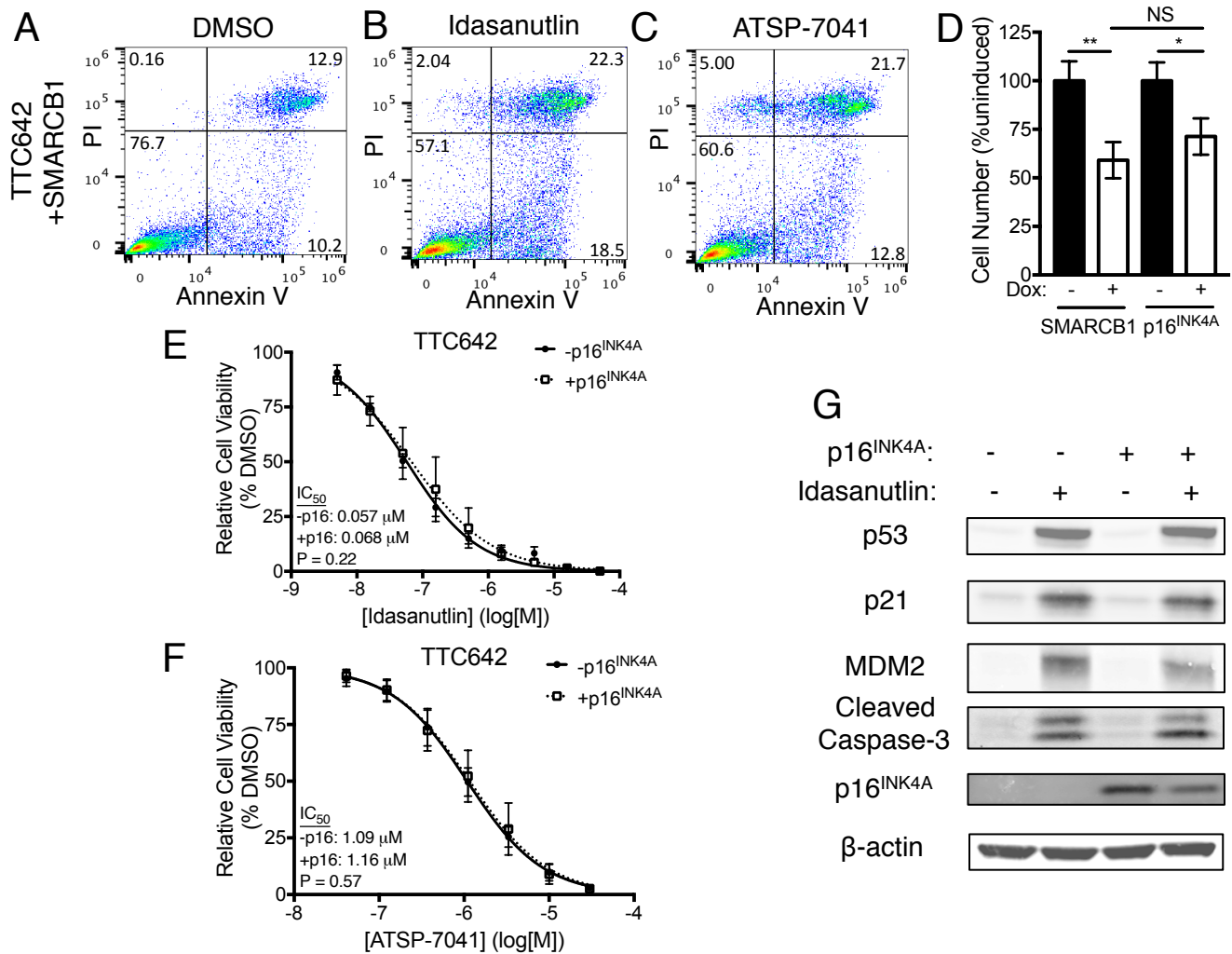
Supplementary Figure 3. Production and characterization of p53-null MRT clones. (A) Gene diagram of *TP53* indicating the locations of the two sgRNAs used to inactivate the gene compared to exons (boxes), introns (lines) and major p53 domains: transactivation – red; DNA binding – blue; C-terminal tetramerization and regulatory region – green. (B) Immunoblot of parental and p53-null clones derived from G401 and MON MRT cells with and without treatment of idasanutlin (1μM for 24h). (C-D) RT-qPCR for *CDKN1A* (encodes p21; C) and *MDM2* (D) in the clones tested in B. Each bar normalized to the corresponding parental line treated with 0.01% DMSO. Error bars represent the standard deviation of three technical replicates. (E) Summary of mutations in each p53-null clone determined through PCR and Sanger sequencing. While the two-sgRNA system was designed to create deletions of the DNA binding domain, other outcomes, including insertions, inversions, and smaller indels at one site are possible. MON cells do not grow in tight colonies, making it difficult to obtain populations derived from a single cell and explaining why three different alleles were detected in some clones.



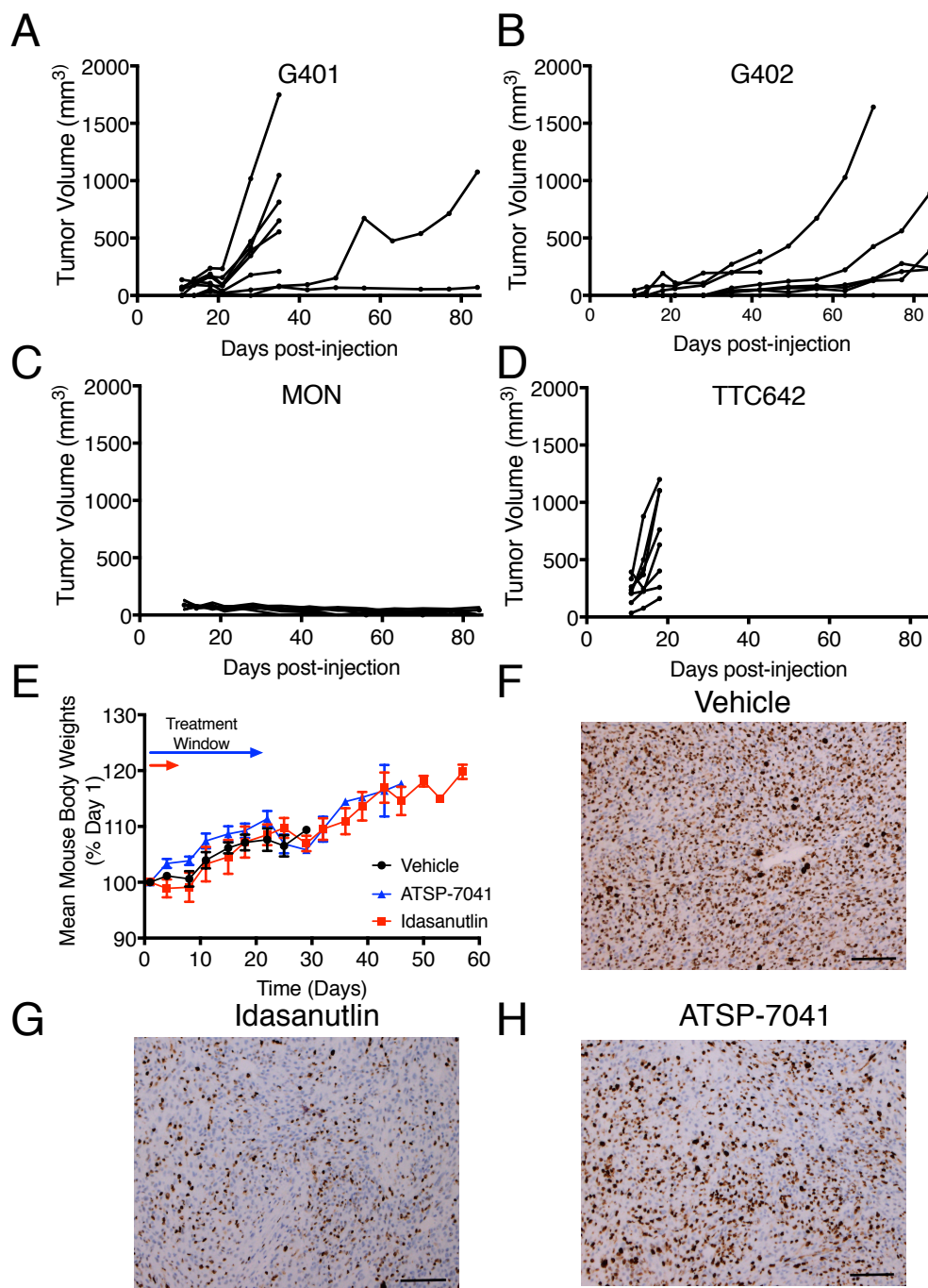
Supplementary Figure 4. MDM2 and MDM2/4 inhibition activates the p53 pathway in MRT cells. (A) Treatment with 1 μ M idasanutlin for 24h in 6 MRT cell lines, 2 p53-null clones of MRT cell lines, and 4 control cell lines while blotting for p53 and two of its target genes, p21 and MDM2, as well as cleaved caspase-3. (B) Treatment with 5 μ M ATSP-7041 for 24h as in A. Images shown are representative of three biological replicates.



Supplementary Figure 5. Cell fate decisions of MRT cell lines following MDM2 and MDM2/4 inhibition. (A-C) MRT cell lines were treated with DMSO (black), 1 μ M idasanutlin (red), or 5 μ M ATSP-7041 (blue) for 72 hrs and cells counted at the indicated times. Negative values indicate a decrease in cell number while positive values indicate an increase in cell number. Error bars indicate the SD of three biological replicates. Significance between treated and DMSO groups calculated by two-way ANOVA with Holm-Sidak's multiple comparisons correction. (D) Cell cycle analysis of G402 and TTC642 cells after treatment with DMSO, 1 μ M idasanutlin, or 5 μ M ATSP-7041 for 24 hrs. Data show mean increase in the percentage of G₀ and G₁ cells in compound-treated cells compared to DMSO-treated cells. Error bars indicate the SD of three biological replicates. Significance calculated with a one-sample *t*-test comparing to 0 with Holm-Sidak's multiple comparisons correction. (E-J) Flow cytometry analysis of G402 (E-G) and TTC642 (H-J) cells treated as in D and stained with Annexin V and propidium iodide (PI). Numbers indicate the percentage of total cells in that quadrant. Plots are representative of three biological replicates. (K) G401 cells as in A-C. (L) G401 cells were treated with the indicated compounds for 72 hrs, replated at equal densities, allowed to recover for 4 days, and then stained for senescence-associated β -galactosidase (blue). Cells shown at 200X magnification. Images are representative fields of three biological replicates. (M) Quantitation of senescent cells shown in L. Fifteen fields at 200X magnification were scored and summed for each biological replicate. Data represent the mean \pm SD of three biological replicates. Significance calculated by one-way ANOVA with Holm-Sidak's multiple comparisons correction. (N) Colony formation assay of G401 cells after drug washout following treatment with the indicated compounds for 72 hrs. Image is representative of three biological replicates. (O) Quantitation of crystal violet extraction from colony formation assay in K. Data represent the mean \pm SD of three biological replicates. Significance calculated by one-way ANOVA with Holm-Sidak's multiple comparisons correction. ** - $P < 0.01$; *** - $P < 0.001$; **** - $P < 0.0001$.



Supplementary Figure 6. Characterization of TTC642 cells expressing SMARCB1 or p16^{INK4A}. (A-C) Flow cytometry analysis of TTC642 cells re-expressing SMARCB1 stained with Annexin V and propidium iodide (PI). Samples were treated with DMSO (A), 1 μ M idasanutlin (B), or 5 μ M ATSP-7041 (C) for 24 hrs. Numbers indicate the percentage of total cells in that quadrant. Plots are representative of three biological replicates. (D) Cell counts after doxycycline-induced expression of SMARCB1 or p16^{INK4A} for 48 hrs. Data represent the mean \pm SD of three biological replicates. Significance calculated by one-way ANOVA with Holm-Sidak's multiple comparisons correction. (E-F) Sensitivity of uninduced and p16^{INK4A} expressing TTC642 MRT cells to idasanutlin (E) and ATSP-7041 (F). Data show mean \pm SD of three biological replicates. Significance calculated using an extra-sum-of-squares F test. (G) Immunoblot for p53 pathway responses to idasanutlin treatment (1 μ M for 24h) in TTC642 cells re-expressing p16^{INK4A}. Images are representative of three biological replicates.



Supplementary Figure 7. MRT xenografts' baseline growth characteristics and pharmacodynamic responses. (A-D) Tumor formation capacities of four MRT cell lines: G401 (A), G402 (B), MON (C), and TTC642 (D). Four mice per cell line were injected in both flanks for a total of 8 tumors, each of which is represented by one line. (E) Mouse body weights for the treatment arms presented in Figure 6. The weight of each mouse on an indicated day was corrected for the tumor volume at that time (estimated $1000 \text{ mm}^3 = 1 \text{ g}$) and then divided by the pre-treatment corrected weight. Each starting point is the mean of $n=8$ mice and error bars show the SEM of the group. (F-H) Representative Ki-67 IHC images of different tumors treated with vehicle (F), idasanutlin (G), or ATSP-7041 (H). Three independent mice per arm were given five doses of the indicated treatment and then euthanized 2h (vehicle and idasanutlin) or 4h (ATSP-7041) following the final treatment. Bar indicates $100 \mu\text{m}$.